Detailed Comparison of Deuterium Quadrupole Profiles between Sphingomyelin and Phosphatidylcholine Bilayers

Tomokazu Yasuda,[†‡] Masanao Kinoshita,[‡] Michio Murata,[†‡] and Nobuaki Matsumori[†*]
[†]Department of Chemistry, Graduate School of Science, Osaka University, Toyonaka, Osaka, Japan; and [‡]Japan Science and Technology Agency, ERATO, Lipid Active Structure Project, Toyonaka, Osaka, Japan

ABSTRACT Lipid rafts are microdomains rich in sphingomyelin (SM) and cholesterol (Chol). The essential question is why natural lipid rafts prefer SM rather than saturated diacyl glycerophosphocholine, although both form ordered membranes with Chol in model systems. Hence in this study, we synthesized site-specifically deuterated 1-palmitoyl-2-stearoyl-*sn*-glycero-3-phosphocholines that match the acyl chain length of stearoyl-SM (SSM), and compared their deuterium quadrupole coupling profiles in detail. The results suggest a deeper distribution of Chol in the SSM membranes, a lower entropic penalty upon accommodation of Chol in SSM membranes, and a higher thermal stability of acyl-chain orders in the SSM-Chol bilayers than in the 1-palmitoyl-2-stearoyl-*sn*-glycero-3-phosphocholine-Chol system at various Chol concentrations. The entropy effect and thermal stability should render SM a more preferred raft constituent than saturated diacyl glycerophosphocholine. Our data also demonstrate that the selective and comprehensive deuteration strategy is indispensable for accurate comparison of order profiles.

INTRODUCTION

Since the lipid raft hypothesis was proposed in the late 1990s (1), lipid rafts have attracted much attention from multidisciplinary researchers because of their significant functional roles in cellular processes including signal transduction, protein sorting, and microbial infection (2–6). The recent definition states that membrane rafts are small (10–200 nm), heterogeneous, highly dynamic membrane domains rich in cholesterol (Chol) and sphingolipids such as sphingomyelin (SM) (7). The physical properties of raft domains appear to be markedly similar to those of a liquid-ordered (L_o) phase, which is characterized by tight packing but relatively high lateral mobility of lipids. In contrast, unsaturated phosphatidylcholines (PCs) are loosely packed, developing a liquid-disordered (L_α) phase that is often segregated from the L_o domain. Although sphingolipids, such as SM and Chol are believed to be essential for the formation of lipid rafts (8–10), the L_o phase was also ascertained to be formed in model membranes containing saturated PCs, such as 1,2-dipalmitoyl-*sn*-glycero-3-phosphocholine, in the presence of Chol (11). This raises an obvious question of why natural lipid rafts prefer SM rather than saturated PC, although both lipids form ordered phases in the presence of Chol. To find an answer to this question, it is essential to examine the difference between SM and PC membranes, particularly in terms of Chol's ordering effect on each membrane.

To date, numerous molecular dynamic simulations and NMR studies of SM and PC membrane systems have been conducted to understand the nature of lipid rafts; however, systematic comparisons between SM and PC membranes with the same acyl chain have been poorly conducted. For sterol-free bilayers, NMR and simulation studies suggested that SM acyl chains are more ordered than PC acyl chains (12,13). This difference in the acyl chain order can allow Chol to preferentially interact with SM over PC because Chol is known to prefer ordered phospholipids (14,15). Alternatively, some studies suggested that SM-Chol membranes are more stabilized than PC-Chol bilayers as a result of direct intermolecular hydrogen bonding or charge paring between SM and Chol (16–22). In contrast, a recent simulation study and NMR experiments revealed a general similarity and no preference for interaction of Chol with SM over PC (23,24). These inconsistent conclusions are largely attributable to the lack of detailed and systematic experimental data comparing SM and PC membranes.

We recently demonstrated accurate local motions encompassing an entire 18:0 SM (stearoyl-SM, SSM, Fig. 1 *a*) molecule (25), which were captured by measuring quadrupole splittings for site-specifically deuterated SSMs. The quadrupole splitting profiles of SM revealed that Chol enhances the order more effectively in the middle regions of alkyl chains than in the shallow regions. However, the acyl chain orders of SSM were not adequately compared with those of saturated PC. Therefore, to elucidate the motional difference between SM and saturated PC membranes, we synthesized site-specifically deuterated 1-palmitoyl-2-stearoyl-*sn*-glycero-3-phosphocholines (PSPCs, Fig. 1 *a*) that share the same acyl chain length as the SSM that we recently reported (25) and compared their order profiles.

MATERIALS AND METHODS

Chemicals

PSPC was purchased from Avanti Polar Lipids (Alabaster, AL). Chol was purchased from Nacalai Tesque (Kyoto, Japan) and deuterium-depleted water was obtained from Isotec (Sigma Aldrich, St. Louis, MO).

Submitted September 18, 2013, and accepted for publication December 26, 2013.

*Correspondence: matsmori@chem.sci.osaka-u.ac.jp

Editor: Klaus Gawrisch.

0006-3495/14/02/0631/8 $2.00

http://dx.doi.org/10.1016/j.bpj.2013.12.034

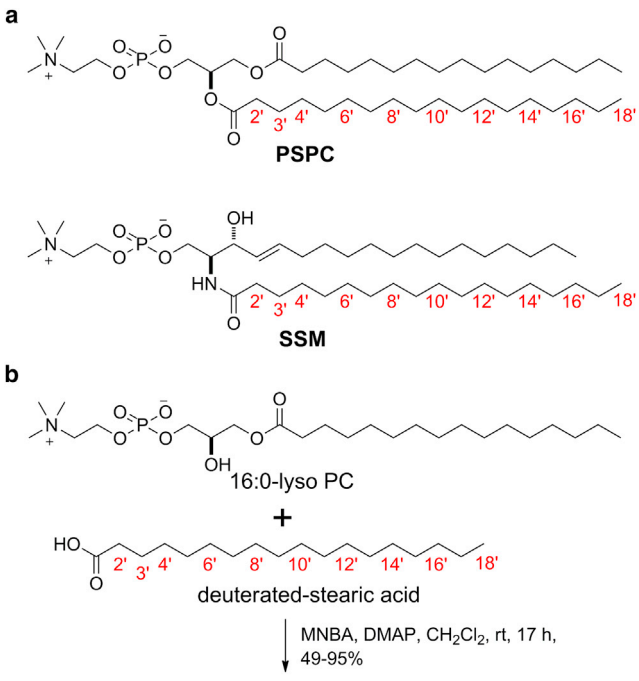

FIGURE 1 Site-specifically deuterated PSPCs. (*a*) Structures of site-specifically deuterated PSPC and SSM. Each numbered position was deuterium labeled. C-18′ was trideuterated and the other positions were dideuterated. (*b*) Synthesis of PSPCs deuterated at *sn*-2 chain. A total of 10 types of deuterium-labeled PSPCs (2′-d_2-, 3′-d_2-, 4′-d_2-, 6′-d_2-, 8′-d_2-, 10′-d_2-, 12′-d_2-, 14′-d_2-, 16′-d_2-, and 18′-d_3-PSPCs) were synthesized to capture the motion of PSPC in bilayers. MNBA: 2-methyl-6-nitrobenzoic anhydride, DMAP: *N*,*N*-dimethyl-4-aminopyridine. To see this figure in color, go online.

Site-specifically deuterated SSMs were synthesized as previously reported (25). Complete experimental details and characterization for site-specifically deuterated PSPC are included in the Supporting Material.

Sample preparation for ^{2}H NMR

For preparation of PSPC membranes, purchased PSPC and deuterated PSPC (10.5 μmol, respectively) were dissolved in methanol-chloroform. For PSPC-Chol samples, Chol (21.0 μmol) was added to the solvent. The solvent was removed in vacuo for at least 12 h. The dried membrane film was hydrated with ~1 mL of water and vigorously vortexed at 65°C to make multilamellar vesicles. After being freeze-thawed three times, each suspension was lyophilized, rehydrated with deuterium-depleted water to be 50% moisture (w/w), and freeze-thawed several times. Each sample was then transferred to a 5-mm glass tube (Wilmad, Vineland, NJ), which was sealed with epoxy glue.

^{2}H NMR measurements

^{2}H NMR spectra were recorded on a 300-MHz CMX300 spectrometer (Chemagnetics, Agilent, Palo Alto, CA) fitted with a 5-mm ^{2}H static probe (Otsuka Electronics, Osaka, Japan) using a quadrupolar echo sequence. The 90° pulse width was 2 μs, the interpulse delay was 30 μs, and the repetition rate was 0.5 s. The sweep width was 200 kHz and the number of scans was ~100,000. ^{2}H NMR spectra and tables of quadrupole splitting values are included in the Supporting Material.

DSC measurements

DSC samples were prepared by a conventional method. Briefly, appropriate amounts of lipid/Chol mixtures dissolved in methanol-chloroform (1:4 v/v) were dried under a flow of nitrogen gas and then in vacuo for >24 h to completely remove the organic solvents. The resulting lipid/Chol mixed films were dispersed in distilled and deionized water and hydrated for 15–20 min at 65°C, which is a higher temperature than the main transition temperature, with intermittent vortexing. Final concentrations of SSM and PSPC were 5.47 and 5.14 mM, respectively. An aliquot of 330 μL of the lipid/Chol suspension was then placed into the nano-differential scanning calorimeter (Diamond, Perkin Elmer, Waltham, MA) immediately before measurements. A scanning rate of 0.2°C/min was used for all DSC measurements.

RESULTS AND DISCUSSION

Synthesis of site-specifically deuterated PSPCs and their ^{2}H quadrupole splitting

A total of 10 types of deuterated PSPCs (2′-d_2-, 3′-d_2-, 4′-d_2-, 6′-d_2-, 8′-d_2-, 10′-d_2-, 12′-d_2-, 14′-d_2-, 16′-d_2-, and 18′-d_3-PSPCs) were synthesized by coupling a series of deuterated stearic acids with 16:0-lyso PC (Fig. 1 *b*). The deuterated stearic acids were synthesized as previously reported (25). Synthetic details for site-specifically deuterated PSPC are given in the Supporting Material.

Next, we measured the ^{2}H NMR spectra of bilayers formed from these deuterated PSPCs and determined the quadrupole splitting values ($\Delta\nu$) in the presence and absence of 50 mol % Chol (Fig. 2 and Fig. S1 in the Supporting Material). Because the phase transition temperature of a pure PSPC membrane is 48.8°C (26), measurements of pure PSPC bilayers were performed at 50°C and 55°C (Fig. 2 *a*), whereas quadrupole splittings were observable even at 20°C in the presence of 50 mol % Chol (Fig. 2 *b*). Interestingly, the ^{2}H NMR profiles of the PSPC acyl chain (Fig. 2), particularly in terms of the effect of Chol, have the same tendency as that of dimyristoylphosphocholine (DMPC) obtained from selectively deuterated DMPC (27), suggesting a general similarity of the order profile of PC membranes irrespective of acyl chain length. On the other hand, it should be noted that this ^{2}H NMR profile of the PC acyl chain (Fig. 2) is different from previously reported order profiles of PC membranes obtained from PCs that bear perdeuterated acyl chains (22,24,28–40). In those studies the overlapped signals from the perdeuterated acyl chains were assigned assuming that the quadrupole splitting decreases monotonically from the lipid-water interface toward the terminus even in the presence of Chol, as presented in Fig. S2. Similar differences between order profiles were also found in SM membranes (13,41,42), as discussed in our previous report (25). This clearly shows that the comprehensive and selective deuteration strategy is necessary for acquiring accurate order profiles.

Comparison with SM membranes

Next, we compared the order profiles of PSPC with those of SSM at 50°C (Fig. 3). In the absence of Chol, the order of

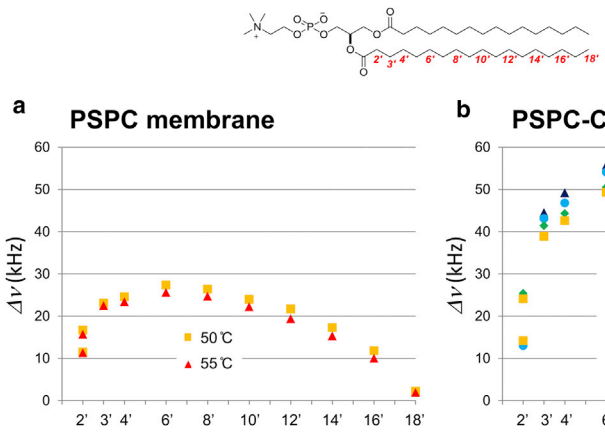

FIGURE 2 Quadrupole splitting profiles of *sn*-2 chain of PSPC at various temperatures. The data were obtained from PSPC membranes in the absence (*a*) and presence (*b*) of 50 mol % Chol. Both membrane samples were hydrated with 50% deuterium-depleted water (w/w). To see this figure in color, go online.

SSM was higher than that of PSPC at each position in the chain (Fig. 3 *c*), with the difference in the C2′–C4′ region being particularly prominent. Because SM has an amide and a hydroxy group that function as both hydrogen bond donors and acceptors, it is generally accepted that these functional groups are involved in intermolecular hydrogen bonding. In fact, we determined the conformation of SM in a membrane environment using bicelles, and found that its conformation is relatively stable and suitable for forming intermolecular hydrogen bonds between the amide groups (43). Therefore, the considerably higher order in the upper acyl chain of SM than in the PC chain (Fig. 3 *c*) may be attributed to the intermolecular hydrogen bonding that restricts the fluctuation and/or changes the orientation of the upper acyl chain of SM.

In contrast to the results obtained with Chol-free PSPC and SSM membranes, the order profiles of SSM-Chol and

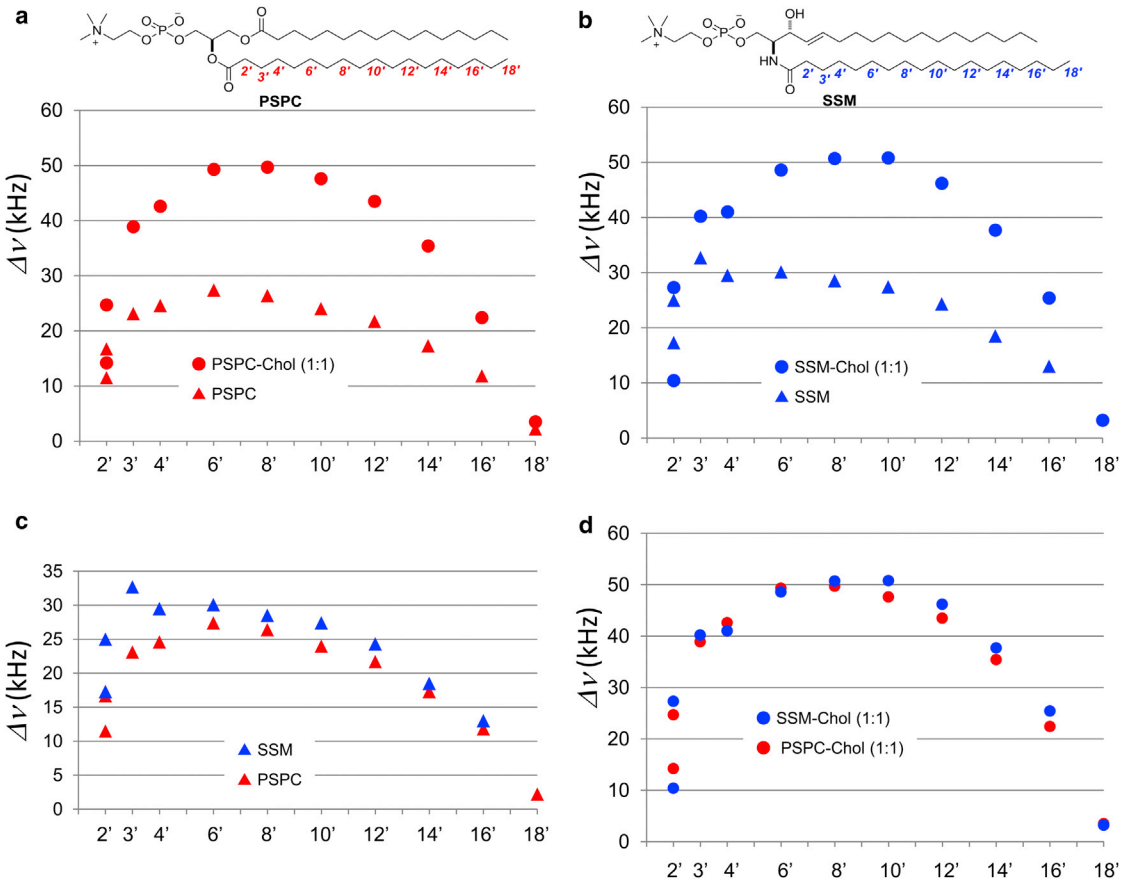

FIGURE 3 Comparison of quadrupole splitting profiles between PSPC and SSM membranes at 50°C. The data were acquired from PSPC (*a*) and SSM (*b*) membranes in the presence (*circles*) and absence (*triangles*) of 50 mol % Chol. Overlaid quadrupole splitting profiles of PSPC (*red*) and SSM (*blue*) membranes in the absence (*c*) and presence (*d*) of 50 mol % Chol. To see this figure in color, go online.

PSPC-Chol membranes appeared to coincide well with each other (Fig. 3 *d*). In fact, previous studies have also pointed out the similarity between SM-Chol and PC-Chol membranes in terms of dynamics and Chol interaction when the acyl chain length is matched (23,24). Nevertheless, our experiments revealed small but significant differences (Fig. 3 *d*); the order is highest at positions C6′–C8′ in PSPC-Chol membranes, whereas it is highest at positions C8′–C10′ in SSM-Chol bilayers, and SSM-Chol bilayers tend to have a slightly higher order in the C10′–C14′ region than PSPC-Chol membranes. To highlight the ordering effect of Chol more clearly, we focused on the difference in quadrupole splitting values between Chol-containing and Chol-free membranes (Fig. 4). This comparison further indicated that the ordering effect of Chol in the upper region of acyl chains (e.g., C3′, C4′, and C6′) is considerably higher in PSPC, whereas in the lower region of the acyl chain (e.g., C14′–C18′), the ordering effect is higher in SSM. Because the rigid alicyclic skeleton of Chol effectively enhances the acyl chain order (44,45), Fig. 4 suggests that the distribution of Chol in PSPC membranes is slightly weighted in the upper region of the acyl chain as compared with the distribution of Chol in SSM membranes. We also calculated the average projected length on the bilayer normal for each segment of the acyl chain (41) to compare the average carbon positions in the membranes (Fig. S3). Accordingly, we found that the cumulative projected chain lengths and the average carbon positions relative to the membrane were completely identical between PSPC-Chol and SSM-Chol bilayers; thus, rationalizing the simple comparison of the vertical position of Chol between PSPC and SSM membranes. Taken together, our data reveal a slightly deeper location of Chol in SSM membranes than in PSPC bilayers. In our previous work (25), we proposed that Chol is more deeply located in SSM membranes than in DMPC membranes, probably because hydrogen bond formation of the polar region of the SM membrane slightly pushes Chol into the membrane interior. Given that Chol is situated beneath the headgroups in PC membranes, thus leading to an umbrella effect (46), the deeper immersion of Chol in SM bilayers than PC bilayers is consistent with the higher umbrella effect of SM membranes. However, there was a significant concern regarding generalizing this notion because of differences in the acyl chain length between SSM and DMPC. The current study shows that this notion holds true for acyl chain-matched SM and saturated PC.

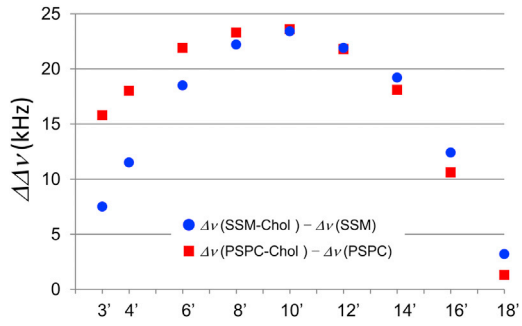

FIGURE 4 Ordering effect of Chol on PSPC and SSM membranes. Figure presents difference in quadrupole splitting values ($\Delta\Delta\nu$) between Chol-containing and Chol-free PSPC (*red squares*) and SSM (*blue circles*) membranes at 50°C. To see this figure in color, go online.

Next, we calculated the area per lipid at 50°C (Table 1) from the order parameters via application of the first-order mean-torque model (31,41) that assumes that the hydrocarbon chains have an average shape of a prism (cylinder or cuboid) in lipid bilayers. The estimated area per SSM is in relatively good agreement with simulated values both in pure and Chol-containing SM membranes (47,48), which validates the model calculation. Comparison of the data (Table 1) reveals that the molecular area of pure SSM (56.6 Å^2) is significantly smaller than that of pure PSPC (60.8 Å^2). This can be also explained by the intermolecular hydrogen bonds between SSM molecules, which compress the mean molecular area of pure SSM more effectively. In contrast, the molecular area was almost identical between SSM-Chol and PSPC-Chol systems (47.6 and 48.0 Å^2), because the highest orders of the acyl chains were comparable. This means that the decrease in molecular area upon accommodation of Chol is smaller in SSM (9.0 Å^2) than in PSPC membrane (12.8 Å^2). In other words, the SSM system can accommodate Chol with a smaller loss of entropy than PSPC membranes, which may partly cause Chol to be more preferentially distributed in SM membranes than PC membranes.

Temperature dependence

Next, we compared the temperature dependence of the quadrupole coupling values of SSM and PSPC at four different depths: C4′, C8′, C12′, and C16′ (Fig. 5). The temperature dependence of SSM-Chol and PSPC-Chol membranes can be approximated by linear functions, as presented in Fig. 5. In the absence of Chol, the difference in temperature dependence was not clear between SSM and PSPC because of inadequate experimental data points. On the other hand, in the presence of Chol the slopes of the approximation lines were steeper in PSPC membranes at any position, demonstrating a larger temperature dependence of PSPC-Chol membranes than SSM-Chol membranes. Notably, the slopes of the approximation lines for PSPC-Chol membranes were markedly steeper at C4′, C12′, and C16′ (Fig. 5, *a*, *c*, and *d*), than at C8′ (Fig. 5 *b*),

TABLE 1 Area per lipid of PSPC and SSM in membranes

	PSPC	PSPC-Chol (1:1)	SSM	SSM-Chol (1:1)
Area-per-lipid (Å^2)	60.8	48.0	56.6	47.6

Calculated via application of the first-order mean-torque model (31,41) from the plateau splittings of the respective membranes at 50°C.

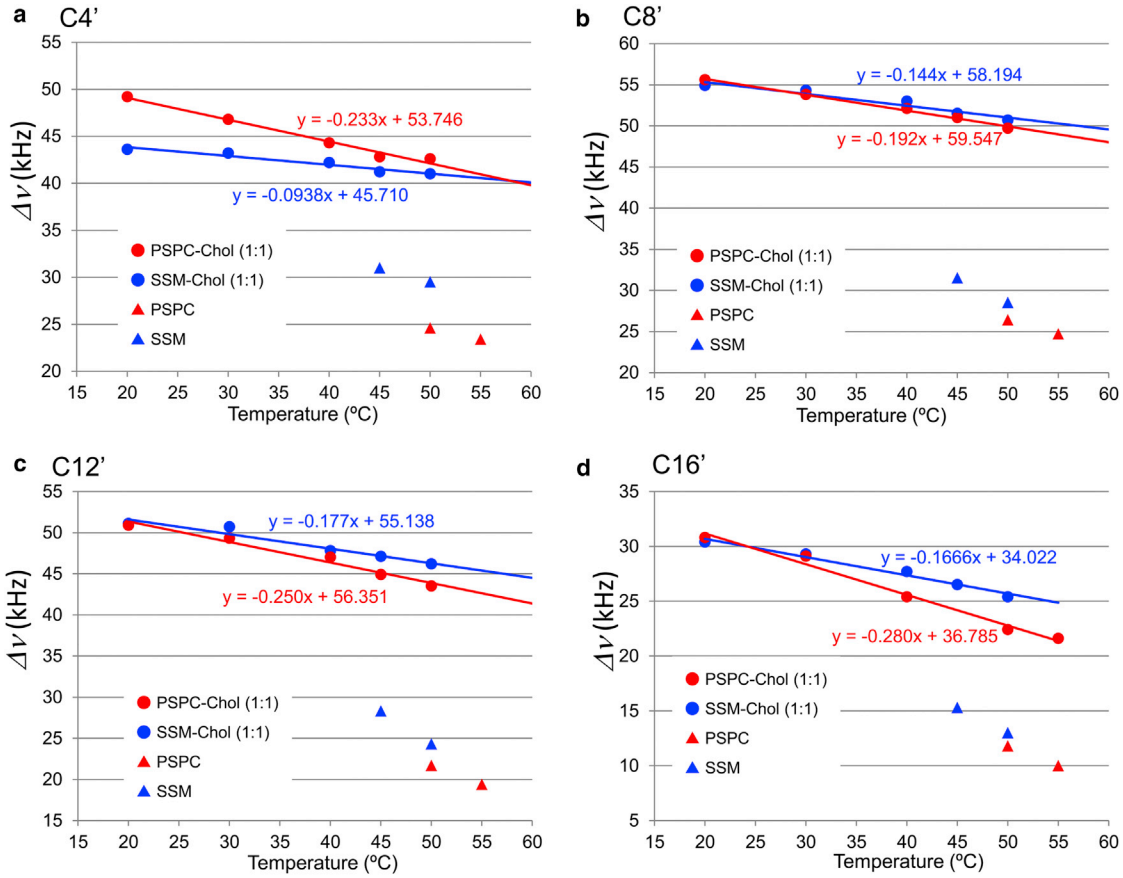

FIGURE 5 Temperature dependence of quadrupole splittings. The quadrupole coupling data were obtained from the C4′ (*a*), C8′ (*b*), C12′ (*c*), and C16′ (*d*) positions of PSPC (*red*) and SSM (*blue*) in the presence and absence of 50 mol % Chol. The temperature dependence of Chol-containing membranes can be linearly approximated, as presented in red and blue lines with approximate equations. To see this figure in color, go online.

indicating that the upper and bottom regions of PSPC acyl chains are more temperature sensitive than the middle regions. The lower temperature sensitivity at C8′ of PSPC-Chol membranes is reasonably accounted for by the presence of rigid Chol rings in that area. In contrast, although the approximation lines in SSM-Chol membranes were generally low-gradient, the slope of the C4′ line (Fig. 5 *a*) was the flattest among them. This can again be interpreted using the notion that hydrogen bonds between SM amides confer higher temperature stability to the upper acyl chain of SSM-Chol membranes.

For further clarification of the differences, we compared the quadrupole coupling values at various molar ratios of Chol. Fig. 6 presents temperature dependence of the quadrupole coupling values for C10′ of SSM and PSPC at 20, 33, and 50 mol % of Chol. Again, SSM membranes exhibited lesser temperature dependence than PSPC membranes at any concentration of Chol, and more importantly, the difference between SSM and PSPC became more prominent with decreasing molar ratios of Chol (Fig. 6, *b* and *c*). These findings showed that SSM-Chol membranes are more tolerant to temperature change, which is more apparent at lower concentrations of Chol.

To correlate the temperature dependence of ^{2}H NMR data with the thermotropic phase behavior of the bilayers, we then measured DSC heating curves of SSM and PSPC bilayers at several molar ratios of Chol. The DSC heating curves (Fig. 7) show that the chain-melting transition progressively decreases in enthalpy and increases in transition width with increases in Chol content, as commonly observed for other SM and PC membranes (49,50), and the transition is abolished completely at 30 mol % of Chol for both PSPC and SSM membranes. According to phase diagrams of binary lipid mixtures with Chol (51), Fig. 7 indicates that both PSPC and SSM membranes containing >30 mol % Chol are in a single L_o phase region, whereas both membranes containing 20 mol % Chol exhibit more complex phase behavior; L_o and gel phases coexist below the sharp component of the chain-melting temperature, and L_α and L_o phases coexist above it. This shows that the phase behaviors are not different between SSM-Chol and PSPC-Chol membranes at the Chol concentrations tested, thus ensuring the direct comparison of the temperature dependence of the order profiles between SSM and PSPC at each Chol concentration (Fig. 6). Taken together, Figs. 6 and 7 reveal that the chain orders in the

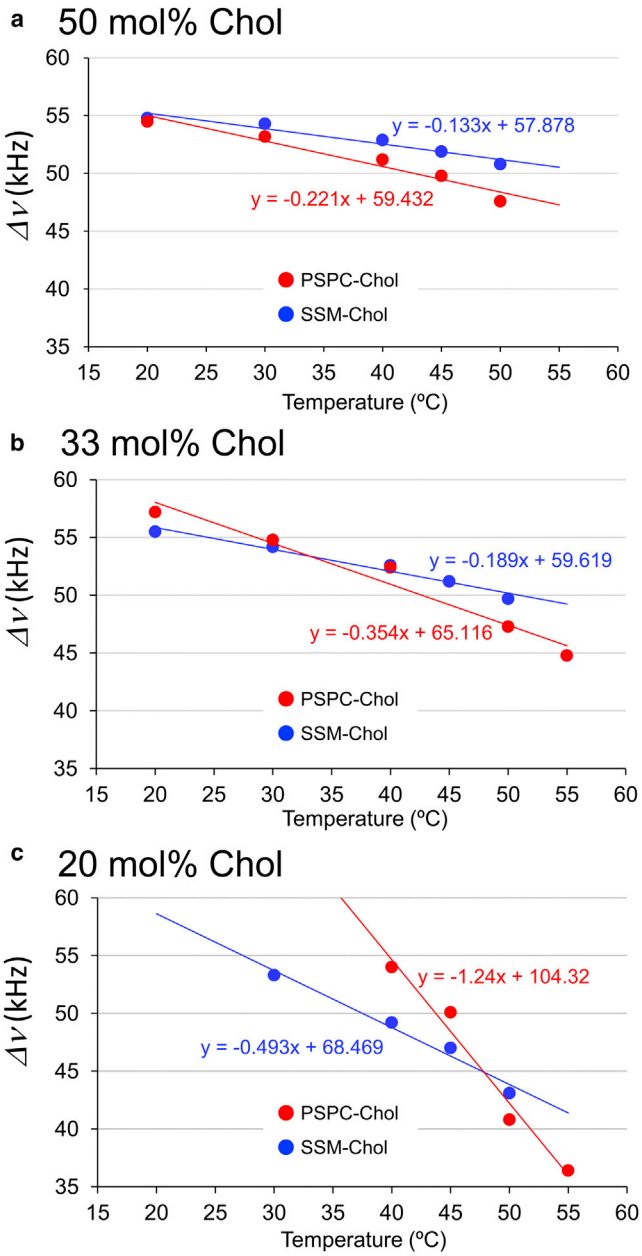

FIGURE 6 Temperature dependence of quadrupole splittings at various Chol concentrations. The quadrupole coupling data were obtained from C10′ of PSPC (*red*) and SSM (*blue*) acyl chains in the presence of Chol at (*a*) 50 mol %, (*b*) 33 mol %, and (*c*) 20 mol %. The temperature dependence of SSM-Chol and PSPC-Chol membranes can be linearly approximated, as presented in red and blue lines with approximation equations. To see this figure in color, go online.

SSM-Chol system are more thermally tolerant than those in the PSPC-Chol system, not only in the single L_o phase region (33 and 50 mol % Chol, Fig. 6, *a* and *b*), but also in more complex phase states (20 mol % Chol, Fig. 6 *c*). From the viewpoint of maintenance of membrane homeostasis, the higher thermal stability of SM-Chol membranes at various Chol concentrations is undoubtedly a favorable property for lipid rafts.

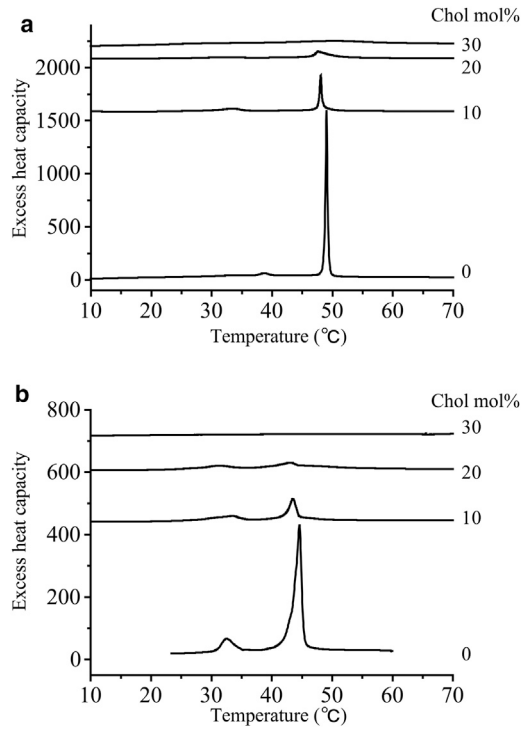

FIGURE 7 DSC heating curves. PSPC (*a*) and SSM (*b*) bilayers containing 0, 10, 20, and 30 mol % Chol.

The next question that needs to be addressed is why the SM-Chol system is more tolerant to temperature change, even at low Chol concentrations. As described previously, SM can form intermolecular hydrogen bonds among SM molecules through their amide groups. In addition, Chol effectively enhances orders in the middle regions of SM acyl chains, as presented in Fig. 3 *b*. Altogether, it is reasonable to suggest that Chol's ordering effect on the acyl chains and the intermolecular hydrogen bond among SM molecules function synergistically to form a more stable ordered phase in the SM-Chol membrane, which leads to robustness against fluctuations in temperature and Chol's concentration.

CONCLUSIONS

It has been difficult to experimentally or theoretically highlight the differences between SM-Chol and PC-Chol systems (23,24); therefore, PC-Chol membranes are often considered equivalent to SM-Chol bilayers in terms of ordered phase formation. In this study, we compared the order profiles of SM and saturated PC using site-specifically deuterated lipids and obtained the following important findings: i), in the absence of Chol, SSM membranes have a higher order than PSPC membranes, in particular for the upper chain region; ii), the difference in ordering effect of Chol suggests a deeper location of Chol in SM membranes; and iii), in terms of acyl-chain order, thermal stability of SSM-Chol membranes is higher than that of PSPC-Chol

membranes, which is more obvious at low Chol concentrations. These findings can be explained by the formation of intermolecular hydrogen bonds between SM molecules. The hydrogen bonds provide a higher order in the upper chain, push Chol into the membrane interior, and assist the formation of a stable ordered membrane at lower concentrations of Chol and over a broader range of temperature. The better thermal tolerance at various Chol ratios, which would arise from the intermolecular hydrogen bonds, should make SM a preferred raft component over saturated PC. In addition, the area per lipid of SSM and PSPC calculated from our order profiles suggested that SSM bilayers can accommodate Chol with a smaller entropic penalty than PSPC, which may be associated with the preferential distribution of Chol toward SM membranes. Thus, this study highlights the small but crucial differences between SM and PC membranes that provide critical clues regarding preference of natural lipid rafts of SM-Chol over PC-Chol systems.

Here, we briefly describe the generality of the current data toward more complicated membrane systems. We very recently observed ^{2}H NMR of deuterated SSM in a ternary membrane system containing SSM, Chol, and unsaturated PC, which is segregated into the L_o and L_α phases (52), and successfully acquired separate quadrupole coupling profiles from each phase, although separated observation of quadrupole splittings from the L_o and L_α phases was already reported using perdeuterated PCs (53). To our surprise, the deuterium quadrupole profile from the L_o phase of the ternary system was almost identical to that in the SM-Chol binary mixture (to be published in due course). This suggests that the order profile from the binary system is essentially applicable to more complicated membrane systems. Detailed comparison of deuterium order profiles in ternary membrane systems containing SSM or PSPC is currently underway.

Although the selective and comprehensive deuteration of acyl chains is not a new strategy but was already applied to DMPC (27), 1,2-dipalmitoyl-*sn*-glycero-3-phosphocholine (54), and other lipids (55,56) in the 1970s, it has been seldom used since then because of the requirement of laborious organic synthesis. On the other hand, perdeuterated lipids are much more frequently used, which have the advantage of allowing a greater range of systems to be studied simultaneously. However, the order profiles obtained in the case of perdeuterated acyl chains are not always sufficient for in-depth analysis of membrane properties due to the ambiguity of assigning overlapped signals. In this context, the selective and comprehensive deuteration strategy of lipid acyl chains is, albeit classical and laborious, indispensable for detailed and accurate comparison of order profiles.

SUPPORTING MATERIAL

Three figures, eleven tables, and general information are available at http://www.biophysj.org/biophysj/supplemental/S0006-3495(14)00003-4.

The authors thank Ms. A. Nakamori, Dr. Y. Umegawa, Dr. N. Inazumi, and Mr. M. Doi, Osaka University, for their help in synthesis and NMR measurements.

This work was supported by Grant-In-Aids for Scientific Research (B) (No. 20310132) and (S) (No. 18101010) from MEXT, Japan, and by SUNBOR grant from Suntory Institute for Bioorganic Research, Japan.

REFERENCES

1. Simons, K., and E. Ikonen. 1997. Functional rafts in cell membranes. *Nature.* 387:569–572.
2. Anderson, R. G. W., and K. Jacobson. 2002. A role for lipid shells in targeting proteins to caveolae, rafts, and other lipid domains. *Science.* 296:1821–1825.
3. Binder, W. H., V. Barragan, and F. M. Menger. 2003. Domains and rafts in lipid membranes. *Angew. Chem. Int. Ed. Engl.* 42:5802–5827.
4. Simons, K., and D. Toomre. 2000. Lipid rafts and signal transduction. *Nat. Rev. Mol. Cell Biol.* 1:31–39.
5. Ikonen, E. 2001. Roles of lipid rafts in membrane transport. *Curr. Opin. Cell Biol.* 13:470–477.
6. Brown, D. A., and E. London. 1998. Functions of lipid rafts in biological membranes. *Annu. Rev. Cell Dev. Biol.* 14:111–136.
7. Pike, L. J. 2006. Rafts defined: a report on the keystone symposium on lipid rafts and cell function. *J. Lipid Res.* 47:1597–1598.
8. Ahmed, S. N., D. A. Brown, and E. London. 1997. On the origin of sphingolipid/cholesterol-rich detergent-insoluble cell membranes: physiological concentrations of cholesterol and sphingolipid induce formation of a detergent-insoluble, liquid-ordered lipid phase in model membranes. *Biochemistry.* 36:10944–10953.
9. Baumgart, T., S. T. Hess, and W. W. Webb. 2003. Imaging coexisting fluid domains in biomembrane models coupling curvature and line tension. *Nature.* 425:821–824.
10. Silvius, J. R., D. del Giudice, and M. Lafleur. 1996. Cholesterol at different bilayer concentrations can promote or antagonize lateral segregation of phospholipids of differing acyl chain length. *Biochemistry.* 35:15198–15208.
11. McMullen, T. P. W., R. N. A. H. Lewis, and R. N. McElhaney. 2004. Cholesterol-phospholipid interactions, the liquid-ordered phase and lipid rafts in model and biological membranes. *Curr. Opin. Colloid Interface Sci.* 8:459–468.
12. Niemelä, P., M. T. Hyvönen, and I. Vattulainen. 2004. Structure and dynamics of sphingomyelin bilayer: insight gained through systematic comparison to phosphatidylcholine. *Biophys. J.* 87:2976–2989.
13. Mehnert, T., K. Jacob, …, K. Beyer. 2006. Structure and lipid interaction of *N*-palmitoylsphingomyelin in bilayer membranes as revealed by ^{2}H-NMR spectroscopy. *Biophys. J.* 90:939–946.
14. Kucerka, N., D. Marquardt, …, J. Katsaras. 2010. Cholesterol in bilayers with PUFA chains: doping with DMPC or POPC results in sterol reorientation and membrane-domain formation. *Biochemistry.* 49:7485–7493.
15. Bennett, W. F., J. L. MacCallum, …, D. P. Tieleman. 2009. Molecular view of cholesterol flip-flop and chemical potential in different membrane environments. *J. Am. Chem. Soc.* 131:12714–12720.
16. Simons, K., and W. L. C. Vaz. 2004. Model systems, lipid rafts, and cell membranes. *Annu. Rev. Biophys. Biomol. Struct.* 33:269–295.
17. Li, X.-M., M. M. Momsen, …, R. E. Brown. 2001. Cholesterol decreases the interfacial elasticity and detergent solubility of sphingomyelins. *Biochemistry.* 40:5954–5963.
18. Bittman, R., C. R. Kasireddy, …, J. P. Slotte. 1994. Interaction of cholesterol with sphingomyelin in monolayers and vesicles. *Biochemistry.* 33:11776–11781.
19. Sankaram, M. B., and T. E. Thompson. 1990. Interaction of cholesterol with various glycerophospholipids and sphingomyelin. *Biochemistry.* 29:10670–10675.

20. Veiga, M. P., J. L. R. Arrondo, …, D. Marsh. 2001. Interaction of cholesterol with sphingomyelin in mixed membranes containing phosphatidylcholine, studied by spin-label ESR and IR spectroscopies. A possible stabilization of gel-phase sphingolipid domains by cholesterol. *Biochemistry.* 40:2614–2622.

21. Aittoniemi, J., P. S. Niemelä, …, I. Vattulainen. 2007. Insight into the putative specific interactions between cholesterol, sphingomyelin, and palmitoyl-oleoyl phosphatidylcholine. *Biophys. J.* 92:1125–1137.

22. Lönnfors, M., J. P. F. Doux, …, J. P. Slotte. 2011. Sterols have higher affinity for sphingomyelin than for phosphatidylcholine bilayers even at equal acyl-chain order. *Biophys. J.* 100:2633–2641.

23. Zhang, Z., S. Y. Bhide, and M. L. Berkowitz. 2007. Molecular dynamics simulations of bilayers containing mixtures of sphingomyelin with cholesterol and phosphatidylcholine with cholesterol. *J. Phys. Chem. B.* 111:12888–12897.

24. Guo, W., V. Kurze, …, J. A. Hamilton. 2002. A solid-state NMR study of phospholipid-cholesterol interactions: sphingomyelin-cholesterol binary systems. *Biophys. J.* 83:1465–1478.

25. Matsumori, N., T. Yasuda, …, M. Murata. 2012. Comprehensive molecular motion capture for sphingomyelin by site-specific deuterium labeling. *Biochemistry.* 51:8363–8370.

26. Lin, H. N., Z. Q. Wang, and C. H. Huang. 1990. Differential scanning calorimetry study of mixed-chain phosphatidylcholines with a common molecular weight identical with diheptadecanoylphosphatidylcholine. *Biochemistry.* 29:7063–7072.

27. Oldfield, E., M. Meadows, …, R. Jacobs. 1978. Spectroscopic studies of specifically deuterium labeled membrane systems. Nuclear magnetic resonance investigation of the effects of cholesterol in model systems. *Biochemistry.* 17:2727–2740.

28. Sankaram, M. B., and T. E. Thompson. 1990. Modulation of phospholipid acyl chain order by cholesterol. A solid-state ^{2}H nuclear magnetic resonance study. *Biochemistry.* 29:10676–10684.

29. Pauls, K. P., A. L. MacKay, and M. Bloom. 1983. Deuterium nuclear magnetic resonance study of the effects of palmitic acid on dipalmitoylphosphatidylcholine bilayers. *Biochemistry.* 22:6101–6109.

30. Penk, A., M. Müller, …, D. Huster. 2011. Structure and dynamics of the lipid modifications of a transmembrane α-helical peptide determined by ^{2}H solid-state NMR spectroscopy. *Biochim. Biophys. Acta.* 1808:784–791.

31. Petrache, H. I., S. W. Dodd, and M. F. Brown. 2000. Area per lipid and acyl length distributions in fluid phosphatidylcholines determined by (2)H NMR spectroscopy. *Biophys. J.* 79:3172–3192.

32. Davis, J. H. 1979. Deuterium magnetic resonance study of the gel and liquid crystalline phases of dipalmitoyl phosphatidylcholine. *Biophys. J.* 27:339–358.

33. Brown, M. F., and A. A. Nevzorov. 1999. ^{2}H-NMR in liquid crystals and membranes. *Colloids Surf. A Physicochem. Eng. Asp.* 158: 281–298.

34. Vermeer, L. S., B. L. de Groot, …, J. Czaplicki. 2007. Acyl chain order parameter profiles in phospholipid bilayers: computation from molecular dynamics simulations and comparison with ^{2}H NMR experiments. *Eur. Biophys. J.* 36:919–931.

35. Thurmond, R. L., G. Lindblom, and M. F. Brown. 1993. Curvature, order, and dynamics of lipid hexagonal phases studied by deuterium NMR spectroscopy. *Biochemistry.* 32:5394–5410.

36. De Boeck, H., and R. Zidovetzki. 1992. Interactions of saturated diacylglycerols with phosphatidylcholine bilayers: a ^{2}H NMR study. *Biochemistry.* 31:623–630.

37. Jamson, M., R. L. Thurmond, …, M. F. Brown. 1992. Deuterium NMR study of intermolecular interactions in lamellar phases containing palmitoyl lysophosphatidylcholine. *J. Phys. Chem.* 96:9532–9544.

38. Salmon, A., S. W. Dodd, …, M. F. Brown. 1987. Configurational statistics of acyl chains in polyunsaturated lipid bilayers from ^{2}H NMR. *J. Am. Chem. Soc.* 109:2600–2609.

39. Trouard, T. P., A. A. Nevzorov, …, M. F. Brown. 1999. Influence of cholesterol on dynamics of dimyristoylphosphatidylcholine bilayers as studied by deuterium NMR relaxation. *J. Chem. Phys.* 110:8802–8818.

40. Endress, E., S. Bayerl, …, T. M. Bayerl. 2002. The effect of cholesterol, lanosterol, and ergosterol on lecithin bilayer mechanical properties at molecular and microscopic dimensions: a solid-state NMR and micropipet study. *Langmuir.* 18:3293–3299.

41. Bartels, T., R. S. Lankalapalli, …, M. F. Brown. 2008. Raftlike mixtures of sphingomyelin and cholesterol investigated by solid-state ^{2}H NMR spectroscopy. *J. Am. Chem. Soc.* 130:14521–14532.

42. Bunge, A., P. Müller, …, D. Huster. 2008. Characterization of the ternary mixture of sphingomyelin, POPC, and cholesterol: support for an inhomogeneous lipid distribution at high temperatures. *Biophys. J.* 94:2680–2690.

43. Yamaguchi, T., T. Suzuki, …, M. Murata. 2012. NMR-based conformational analysis of sphingomyelin in bicelles. *Bioorg. Med. Chem.* 20:270–278.

44. Mihailescu, M., R. G. Vaswani, …, S. H. White. 2011. Acyl-chain methyl distributions of liquid-ordered and -disordered membranes. *Biophys. J.* 100:1455–1462.

45. Silvius, J. R. 2003. Role of cholesterol in lipid raft formation: lessons from lipid model systems. *Biochim. Biophys. Acta.* 1610:174–183.

46. Brown, M. F., and J. Seelig. 1978. Influence of cholesterol on the polar region of phosphatidylcholine and phosphatidylethanolamine bilayers. *Biochemistry.* 17:381–384.

47. Khelashvili, G. A., and H. L. Scott. 2004. Combined Monte Carlo and molecular dynamics simulation of hydrated 18:0 sphingomyelin-cholesterol lipid bilayers. *J. Chem. Phys.* 120:9841–9847.

48. Robinson, D. 2013. A polarizable force-field for membrane raft components. *J. Chem. Theory Comput.* 9:2498–2503.

49. McMullen, T. P., R. N. Lewis, and R. N. McElhaney. 1993. Differential scanning calorimetric study of the effect of cholesterol on the thermotropic phase behavior of a homologous series of linear saturated phosphatidylcholines. *Biochemistry.* 32:516–522.

50. Estep, T. N., D. B. Mountcastle, …, T. E. Thompson. 1979. Thermal behavior of synthetic sphingomyelin-cholesterol dispersions. *Biochemistry.* 18:2112–2117.

51. Marsh, D. 2010. Liquid-ordered phases induced by cholesterol: a compendium of binary phase diagrams. *Biochim. Biophys. Acta.* 1798:688–699.

52. Veatch, S. L., and S. L. Keller. 2005. Miscibility phase diagrams of giant vesicles containing sphingomyelin. *Phys. Rev. Lett.* 94:148101-1–148101-4.

53. Veatch, S. L., I. V. Polozov, …, S. L. Keller. 2004. Liquid domains in vesicles investigated by NMR and fluorescence microscopy. *Biophys. J.* 86:2910–2922.

54. Seelig, A., and J. Seelig. 1974. The dynamic structure of fatty acyl chains in a phospholipid bilayer measured by deuterium magnetic resonance. *Biochemistry.* 13:4839–4845.

55. Seelig, J., and J. L. Browning. 1978. General features of phospholipid conformation in membranes. *FEBS Lett.* 97:41–44.

56. Seelig, A., and J. Seelig. 1977. Effect of a single *cis* double bond on the structures of a phospholipid bilayer. *Biochemistry.* 16:45–50.

Supporting Materials

Detailed Comparison of Deuterium Quadrupole Profiles between Sphingomyelin and Phosphatidylcholine Bilayers

Tomokazu Yasuda,[†‡] Masanao Kinoshita,[‡] Michio Murata,[†‡] and Nobuaki Matsumori[†*]

[†] Department of Chemistry, Graduate School of Science, Osaka University, Toyonaka, Osaka 560-0043, Japan.

[‡] Japan Science and Technology Agency, ERATO, Lipid Active Structure Project, Toyonaka, Osaka 560-0043, Japan.

Supplementary Method

General information for synthesis:

1-palmitoyl-2-hydroxy-sn-glycero-3-phosphocholine was purchased from Avanti Polar Lipids. Other chemicals and solvents were purchased from Nacalai Tesque, Aldrich, TCI, and KANTO Chemicals Inc., and used without further purification unless otherwise noted. Thin layer chromatography and column chromatography were Merck precoated silica gel 60 F-254 plates and silica gel 60 (100-200 um), respectively. Proton nuclear magnetic resonance spectra were collected on a JEOL ECA 500 (500 MHz) or a JEOL ECS 400 (400 MHz). Mass spectrometry was performed using LCQ-DECA (Tharmo quest), and high resolution mass spectra (HRMS) were recorded on a LTQ-Orbitrap XL. Voltex mixers of VOLTEX-2GENIE (scientific industries) and ultrasonic cleaner BRANSON 1510 (Yamato Inc.) were used for liposome preparation. A series of deuterated stearic acids (2-d_2-, 3-d_2-, 4-d_2-, 6-d_2-, 8-d_2-, 10-d_2-, 12-d_2-, 14-d_2-, 16-d_2-, 18-d_3-stearic acids**)** were synthesized as previously reported (1).

Synthesis of 2'-d_2-, 3'-d_2-, 4'-d_2-, 6'-d_2-, 8'-d_2-, 10'-d_2-, 12'-d_2-, 14'-d_2-, 16'-d_2-, and 18'-d_3-PSPCs

To a solution of 1-palmitoyl-2-hydroxy-sn-glycero-3-phosphocholine (52.1 mg, 0.11 mmol) and deuterated stearic acid (41.1 mg, 0.14 mmol) in dichlorometane (3.0 ml) were added 2-methyl-6-nitrobenzoic anhydride (189 mg, 0.55 mmol), *N*,*N*-dimethyl-4-aminopyridine (134 mg, 1.10 mmol). After the reaction mixture was stirred for 17 h at room temperature, the reaction was quenched with MeOH, and solvent was evaporated to give the crude products. Purification by silica gel column chromatography ($CHCl_3$/MeOH = 3/1 to $CHCl_3$/MeOH/H_2O = 65/25/4) afforded 2'-d_2-PSPC as white solids. 3'-d_2-, 4'-d_2-, 6'-d_2-, 8'-d_2-, 10'-d_2-, 12'-d_2-, 14'-d_2-, 16'-d_2-, and 18'-d_3-PSPCs were prepared from respective deuterated stearic acid in a similar manner.

2'-d_2-PSPC: white solid (52.9 mg, 0.07 mmol, 63%). R_f 0.70 (silica gel, $CHCl_3$/MeOH/H_2O = 65/35/8); ^{1}H NMR (400 MHz, CD_3OD) δ 5.24 (1H, br, H2), 4.41 (1H, dd, *J* = 12.4, 3.2 Hz, H1), 4.25

(2H, br, α), 4.15 (1H, dd, *J* = 12.0, 6.8 Hz, H1), 3.98 (2H, t, *J* = 6.4 Hz, H3), 3.62 (2H, t, *J* = 4.8 Hz, β), 3.21 (9H, s, -N^+Me_3), 2.30 (71%*, br, H2'), 2.01 (4H, t, *J* = 6.4 Hz , H3'), 1.27 (50H, s, -CH_2-), 0.88 (6H, t, *J* = 6.4 Hz,H18, H18') *not deuterated H (%); ESI-HRMS m/z calcd for $C_{42}H_{82}D_2NO_8PNa^+$ $(M+Na)^+$ 786.5952, found 786.5946**.**

3'-*d*$_2$-PSPC: white solid (38.7 mg, 0.05 mmol, 50%). R_f 0.67 (silica gel, $CHCl_3$/MeOH/H_2O = 65/35/8); ^{1}H NMR (400 MHz, CD_3OD) δ 5.25 (1H, br, H2), 4.41 (1H, dd, *J* = 12.4, 3.2 Hz, H1), 4.25 (2H, br, α), 4.15 (1H, dd, *J* = 12.0, 6.8 Hz, H1), 3.98 (2H, t, *J* = 6.3 Hz, H3), 3.62 (2H, t, *J* = 4.8 Hz, β), 3.21 (9H, s, -N^+Me_3), 2.30 (4H, br, H2'), 2.01 (66%*, br, H3'), 1.25 (50H, s, -CH_2-), 0.88 (6H, t, *J* = 6.4 Hz,H18, H18') *not deuterated H (%); ESI-HRMS m/z calcd for $C_{42}H_{82}D_2NO_8PNa^+$ $(M+Na)^+$ 786.5952, found 786.5946**.**

4'-*d*$_2$-PSPC: white solid (44.8 mg, 0.06 mmol, 49%). R_f 0.71 (silica gel, $CHCl_3$/MeOH/H_2O = 65/35/8); ^{1}H NMR (400 MHz, CD_3OD) δ 5.25 (1H, br, H2), 4.40 (1H, dd, *J* = 12.4, 3.2 Hz, H1), 4.25 (2H, br, α), 4.15 (1H, dd, *J* = 12.0, 6.8 Hz, H1), 3.98 (2H, t, *J* = 6.3 Hz, H3), 3.62 (2H, t, *J* = 4.8 Hz, β), 3.20 (9H, s, -N^+Me_3), 2.30 (4H, br, H2'), 2.01 (4H, br, H3'), 1.24 (48H, s, -CH_2-), 0.88 (6H, t, *J* = 6.4 Hz,H18, H18'); ESI-HRMS m/z calcd for $C_{42}H_{82}D_2NO_8PNa^+$ $(M+Na)^+$ 786.5952, found 786.5952**.**

6'-*d*$_2$-PSPC: white solid (72.6 mg, 0.09 mmol, 90%). R_f 0.69 (silica gel, $CHCl_3$/MeOH/H_2O = 65/35/8); ^{1}H NMR (400 MHz, CD_3OD) δ 5.25 (1H, br, H2), 4.41 (1H, dd, *J* = 12.4, 3.2 Hz, H1), 4.24 (2H, br, α), 4.15 (1H, dd, *J* = 12.0, 6.8 Hz, H1), 3.98 (2H, t, *J* = 6.3 Hz, H3), 3.62 (2H, t, *J* = 4.8 Hz, β), 3.20 (9H, s, -N^+Me_3), 2.30 (4H, br, H2'), 2.01 (4H, br, H3'), 1.25 (48H, s, -CH_2-), 0.88 (6H, t, *J* = 6.4 Hz,H18, H18'); ESI-HRMS m/z calcd for $C_{42}H_{82}D_2NO_8PNa^+$ $(M+Na)^+$ 786.5952, found 786.5958**.**

8'-d_2-PSPC: white solid (70.0 mg, 0.09 mmol, 90%). R_f 0.70 (silica gel, $CHCl_3$/MeOH/H_2O = 65/35/8); ^{1}H NMR (400 MHz, CD_3OD) δ 5.25 (1H, br, H2), 4.41 (1H, dd, *J* = 12.4, 3.2 Hz, H1), 4.24 (2H, br, α), 4.15 (1H, dd, *J* = 12.0, 6.8 Hz, H1), 3.98 (2H, t, *J* = 6.3 Hz, H3), 3.62 (2H, t, *J* = 4.8 Hz, β), 3.21 (9H, s, -N^+Me_3), 2.30 (4H, br, H2'), 2.01 (4H, br, H3'), 1.25 (48H, s, -CH_2-), 0.88 (6H, t, *J* = 6.4 Hz,H18, H18'); ESI-HRMS m/z calcd for $C_{42}H_{82}D_2NO_8PNa^+$ $(M+Na)^+$ 786.5952, found 786.5960**.**

10'-d_2-PSPC: white solid (74.0 mg, 0.10 mmol, 95%). R_f 0.71 (silica gel, $CHCl_3$/MeOH/H_2O = 65/35/8); ^{1}H NMR (400 MHz, CD_3OD) δ 5.25 (1H, br, H2), 4.41 (1H, dd, *J* = 12.4, 3.2 Hz, H1), 4.24 (2H, br, α), 4.15 (1H, dd, *J* = 12.0, 6.8 Hz, H1), 3.98 (2H, t, *J* = 6.3 Hz, H3), 3.62 (2H, t, *J* = 4.8 Hz, β), 3.21 (9H, s, -N^+Me_3), 2.31 (4H, br, H2'), 2.01 (4H, br, H3'), 1.24 (48H, s, -CH_2-), 0.88 (6H, t, *J* = 6.4 Hz,H18, H18'); ESI-HRMS m/z calcd for $C_{42}H_{82}D_2NO_8PNa^+$ $(M+Na)^+$ 786.5952, found 786.5961**.**

12'-d_2-PSPC: white solid (70.9 mg, 0.09 mmol, 92%). R_f 0.70 (silica gel, $CHCl_3$/MeOH/H_2O = 65/35/8); ^{1}H NMR (400 MHz, CD_3OD) δ 5.25 (1H, br, H2), 4.41 (1H, dd, *J* = 12.4, 3.2 Hz, H1), 4.24 (2H, br, α), 4.15 (1H, dd, *J* = 12.0, 6.8 Hz, H1), 3.98 (2H, t, *J* = 6.3 Hz, H3), 3.61 (2H, t, *J* = 4.8 Hz, β), 3.21 (9H, s, -N^+Me_3), 2.31 (4H, br, H2'), 2.01 (4H, br, H3'), 1.25 (48H, s, -CH_2-), 0.88 (6H, t, *J* = 6.4 Hz,H18, H18'); ESI-HRMS m/z calcd for $C_{42}H_{82}D_2NO_8PNa^+$ $(M+Na)^+$ 786.5952, found 786.5960**.**

14'-d_2-PSPC: white solid (65.6 mg, 0.09 mmol, 83%). R_f 0.71 (silica gel, $CHCl_3$/MeOH/H_2O = 65/35/8); ^{1}H NMR (400 MHz, CD_3OD) δ 5.25 (1H, br, H2), 4.41 (1H, dd, *J* = 12.4, 3.2 Hz, H1), 4.24 (2H, br, α), 4.15 (1H, dd, *J* = 12.0, 6.8 Hz, H1), 3.98 (2H, t, *J* = 6.3 Hz, H3), 3.60 (2H, t, *J* = 4.8 Hz, β), 3.20 (9H, s, -N^+Me_3), 2.31 (4H, br, H2'), 2.01 (4H, br, H3'), 1.25 (48H, s, -CH_2-), 0.88 (6H, t, *J* = 6.4 Hz,H18, H18'); ESI-HRMS m/z calcd for $C_{42}H_{82}D_2NO_8PNa^+$ $(M+Na)^+$ 786.5952, found 786.5960**.**

16'-d_2-PSPC: white solid (65.0 mg, 0.08 mmol, 58%). R_f 0.71 (silica gel, $CHCl_3$/MeOH/H_2O = 65/35/8); ^{1}H NMR (400 MHz, CD_3OD) δ 5.25 (1H, br, H2), 4.41 (1H, dd, *J* = 12.4, 3.2 Hz, H1), 4.24 (2H, br, α), 4.15 (1H, dd, *J* = 12.0, 6.8 Hz, H1), 3.98 (2H, t, *J* = 6.3 Hz, H3), 3.60 (2H, t, *J* = 4.8 Hz, β), 3.20 (9H, s, -N^+Me_3), 2.31 (4H, br, H2'), 2.01 (4H, br, H3'), 1.25 (48H, s, -CH_2-), 0.88 (6H, t, *J* = 6.4 Hz,H18, H18'); ESI-HRMS m/z calcd for $C_{42}H_{82}D_2NO_8PNa^+$ $(M+Na)^+$ 786.5952, found 786.5958**.**

18'-d_3-PSPC: white solid (54.7 mg, 0.07 mmol, 86%). R_f 0.71 (silica gel, $CHCl_3$/MeOH/H_2O = 65/35/8); ^{1}H NMR (400 MHz, CD_3OD) δ 5.25 (1H, br, H2), 4.41 (1H, dd, *J* = 12.4, 3.2 Hz, H1), 4.24 (2H, br, α), 4.15 (1H, dd, *J* = 12.0, 6.8 Hz, H1), 3.98 (2H, t, *J* = 6.3 Hz, H3), 3.60 (2H, t, *J* = 4.8 Hz, β), 3.20 (9H, s, -N^+Me_3), 2.31 (4H, br, H2'), 2.01 (4H, br, H3'), 1.25 (50H, s, -CH_2-), 0.88 (3H, t, *J* = 6.4 Hz,H18); ESI-HRMS m/z calcd for $C_{42}H_{81}D_3NO_8PNa^+$ $(M+Na)^+$ 787.6015, found 787.6024**.**

Supplementary Figures

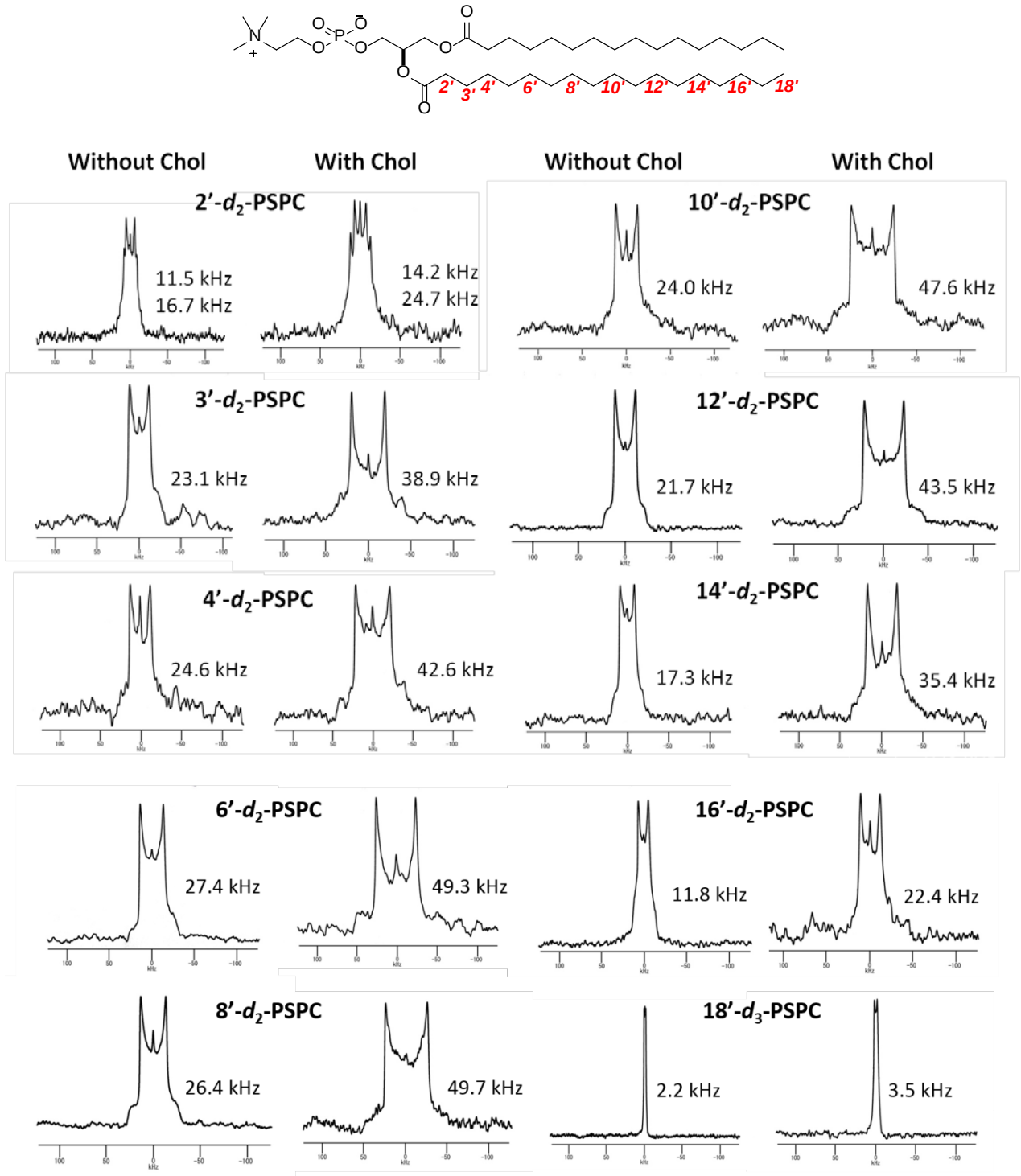

Figure S1. ^{2}H NMR spectra of deuterated PSPC bilayers in the oresence and absence of 50 mol% Chol at 50 ºC. To conserve the amount of deuterated PSPCs, we mixed commercially available unlabeled PSPC.

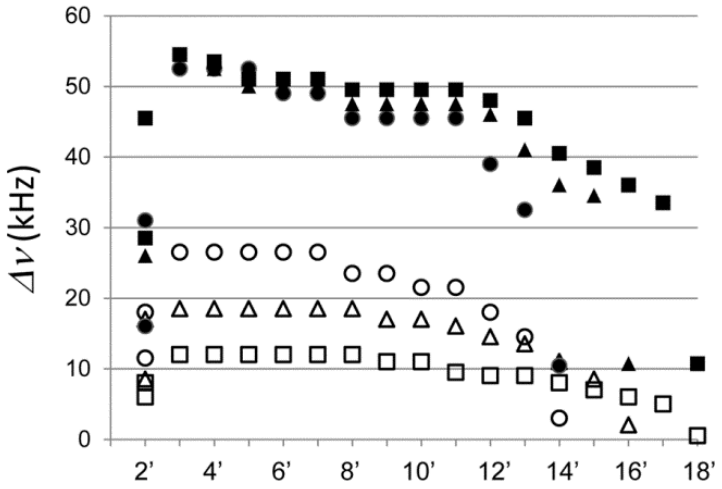

Figure S2. Reported quadrupole splitting profiles of *sn*-2 chain of DMPC, DPPC, and DSPC determined from perdeuterated acyl chains. The data were obtained from DMPC-d_{54} (○, ●), DPPC-d_{62} (△, ▲), and DSPC-d_{70} (□, ■) in the presence (●, ▲, ■) and absence (○, Δ, □) of 50 mol% Chol, at 35 °C for DMPC-d_{54}, at 52 °C for DPPC-d_{62}, and at 63 °C for DSPC-d_{70}. Data from Supporting Ref 2.

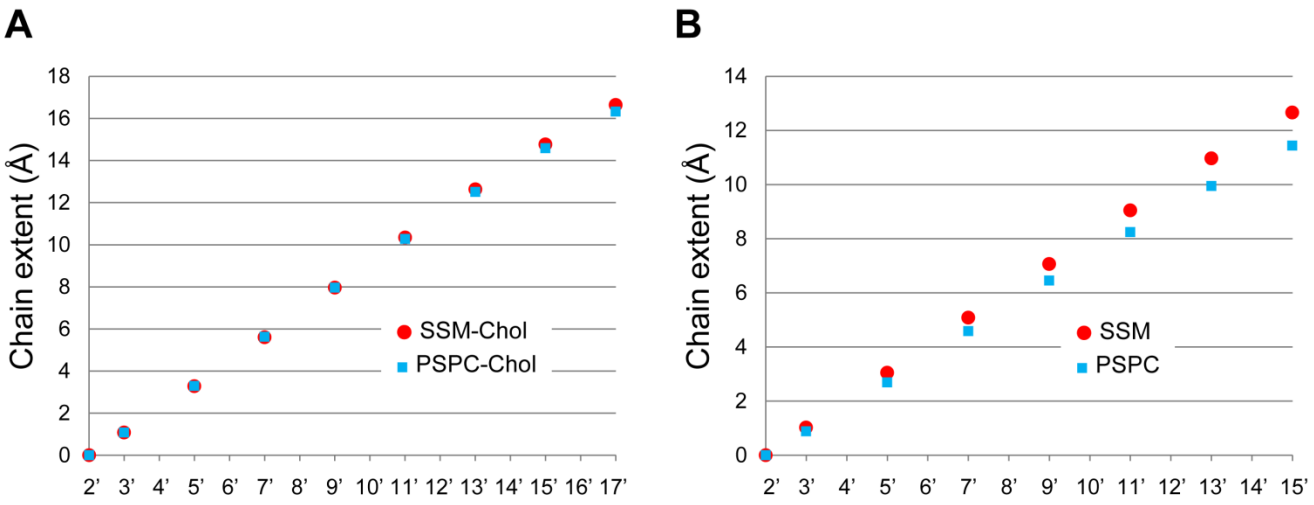

Figure S3. Segmental projections onto the bilayer normal for Chol-containing (A) and pure (B) bilayers at 50 ºC. The calculation was made from quadrupole splitting values on the basis of the first-order mean-torque model (3). The abscissa axes start from the C2' carbon, and end at the C17' carbon for cholesterol-containing membranes (A) and at the C15' carbon for pure PSPC and SSM membranes (B). The reason why the abscissa axes don't terminate at the C18' carbon is that we don't have the order parameter of C17' that is necessary to obtain the full chain projection including C18'. In addition, since the absolute values of order parameters of the C16' for pure SSM and PSPC membranes are below 0.125 that is the criteria for the application of the first-order mean-torque model, the abscissa ends at the C15' carbon in panel B.

Supplementary Tables

Table S1. Quadrupolar couplings (kHz) of 2'-d_2-PSPC membranes

	PSPC	PSPC/Chol
20 °C	-	-
30 °C	-	13.0, 24.7
40 °C	-	14.0, 25.4
50 °C	11.5, 16.7	14.2, 24.7
55 °C	11.3, 15.7	14.4, 24.1

Table S2. Quadrupolar couplings (kHz) of 3'-d_2-PSPC membranes

	PSPC	PSPC/Chol
20 °C	-	44.5
30 °C	-	43.1
40 °C	-	41.4
50 °C	23.1	38.9
55 °C	22.5	37.9

Table S3. Quadrupolar couplings (kHz) of 4'-d_2-PSPC membranes

	PSPC	PSPC/Chol
20 °C	-	49.2
30 °C	-	46.8
40 °C	-	44.3
50 °C	24.6	42.6
55 °C	23.4	

Table S4. Quadrupolar couplings (kHz) of 6'-d_2-PSPC membranes

	PSPC	PSPC/Chol
20 °C	-	55.7
30 °C	-	54.1
40 °C	-	50.5
50 °C	27.4	49.3
55 °C	25.6	48.0

Table S5. Quadrupolar couplings (kHz) of 8'-d_2-PSPC membranes

	PSPC	PSPC/Chol
20 °C	-	55.6
30 °C	-	53.8
40 °C	-	52.1
50 °C	26.4	49.7
55 °C	24.7	

Table S6. Quadrupolar couplings (kHz) of 10'-d_2-PSPC membranes

	PSPC	PSPC/Chol (50 mol%)	PSPC/Chol (33 mol%)	PSPC/Chol (20 mol%)
20 °C	-	52.1	57.2	-
30 °C	-	53.2	54.8	-
40 °C	-	51.2	52.4	54.0
45 °C	-	49.8		54.0
50 °C	24.0	47.6	48.3	40.8
55 °C	22.2		44.8	36.4

Table S7. Quadrupolar couplings (kHz) of 12'-d_2-PSPC membranes

	PSPC	PSPC/Chol
20 °C	-	50.9
30 °C	-	49.3
40 °C	-	47.0
50 °C	21.7	43.5
55 °C	19.4	

Table S8. Quadrupolar couplings (kHz) of 14'-d_2-PSPC membranes

	PSPC	PSPC/Chol
20 °C	-	44.2
30 °C	-	41.0
40 °C	-	38.1
50 °C	17.3	35.4
55 °C	15.3	34.4

Table S9. Quadrupolar couplings (kHz) of 16'-d_2-PSPC membranes

	PSPC	PSPC/Chol
20 °C	-	30.8
30 °C	-	29.1
40 °C	-	25.4
50 °C	11.8	22.4
55 °C	10.0	21.6

Table S10. Quadrupolar couplings (kHz) of 18'-d_3-PSPC membranes

	PSPC	PSPC/Chol
20 °C	-	5.6
30 °C	-	4.8
40 °C	-	4.3
50 °C	2.2	3.5
55 °C	1.9	2.9

Table S11. Quadrupolar couplings (kHz) of 10'-d_2-SSM membranes

	SSM/Chol (50 mol%)	SSM/Chol (33 mol%)	SSM/Chol (20 mol%)
20 °C	54.8	55.5	-
30 °C	54.3	54.2	53.3
40 °C	52.9	52.6	49.2
45 °C	51.9	51.2	47.0
50 °C	50.8	49.8	43.1

Supporting References

1. Matsumori, N., T. Yasuda, H. Okazaki, T. Suzuki, T. Yamaguchi, H. Tsuchikawa, M. Doi, T. Oishi, and M. Murata. 2012. Comprehensive molecular motion capture for sphingomyelin by site-specific deuterium labeling. *Biochemistry.* 51:8363–8370.
2. Sankaram, M. B., and T. E. Thompson. 1990. Modulation of phospholipid acyl chain order by cholesterol. A solid-state ^{2}H nuclear magnetic resonance study. *Biochemistry.* 29:10676–10684.
3. Bartels, T., R. S. Lankalapalli, R. Bittman, K. Beyer, and M. F. Brown. 2008. Raftlike mixtures of sphingomyelin and cholesterol investigated by solid-state ^{2}H NMR spectroscopy. *J Am Chem Soc.* 130:14521–14532.